NASA

Technical Memorandum **79657**

Operational Modes for a Wave Injection Facility Aboard Spacelab and a Sub-Satellite

Peter L. Dyson

SEPTEMBER 1978

National Aeronautics and
Space Administration

Goddard Space Flight Center
Greenbelt, Maryland 20771

TM 79657

OPERATIONAL MODES FOR A WAVE INJECTION FACILITY ABOARD SPACELAB AND A SUB-SATELLITE

Peter L. Dyson*

September 1978

NASA/Goddard Space Flight Center
Laboratory for Planetary Atmospheres
Greenbelt, Maryland 20771

*NAS/NRC Resident Research Associate

OPERATIONAL MODES FOR A WAVE INJECTION FACILITY ABOARD SPACELAB AND A SUB-SATELLITE

Peter L. Dyson*

ABSTRACT

The Spacelab program offers an opportunity to put a sophisticated Wave Injection Facility into orbit to study many aspects of space plasmas. Such a facility would cover a very wide frequency range including MF and HF. In the Alouette and ISIS programs experiments were also done at these frequencies. Significant technical developments have been made since then, however, and it is now possible to carry out more extensive measurements on the properties of waves propagating in the space plasma. For instance, phase and Doppler shift measurements can be made to give more accurate measurements of echo time delay and the angle of arrival. This report examines various modes of operation of a Wave Injection Facility in order to demonstrate the type of measurements which can be made. Since the Spacelab flights will involve sub-satellites, some consideration is given to propagation between two vehicles both at HF and VHF.

*NAS/NRC Resident Research Associate

CONTENTS

CONTENTS (Continued)

ILLUSTRATIONS

ILLUSTRATIONS (Continued)

OPERATIONAL MODES FOR A WAVE INJECTION FACILITY ABOARD SPACELAB AND A SUB-SATELLITE

1. Introduction

This report considers the operation of a Wave Injection Facility primarily from the point of view of measuring the properties of electromagnetic signals in the MF and HF bands. The modes of operation suggested need not, however, be restricted to these types of singal and can be used in other frequency ranges and for other types of signals (such as electrostatic waves associated with plasma resonances). It should also be noted that the operating modes suggested here are not necessarily the only desirable modes at MF and HF. They are meant to be basic general purpose modes of operation which will yield a considerable amount of useful information. In fact, other modes of operation (or variations of the modes discussed here) will also be used for certain studies. However, it is felt that the operating modes presented are sufficient to illustrate the MF and HF capabilities of the proposed facility.

It should be understood that the type of computer controlled facility discussed here offers great flexibility in designing modes of operation and that new operating modes can be implemented at any time simply by writing a new control program, i.e., only changes in software are required. This type of computer controlled operation has proven successful with ground based ionosondes (e.g. Bibl and Reinisch, 1978; Devlin, 1978). The development of the Wave Injection Facility will be evolutionary i . nature and a flexible computer controlled facility is consistent with that philosophy.

A specific case of combining HF and VHF measurements to measure properties of gravity waves is discussed. Again, this is an illustrative example and is not meant to exclude other modes of combined operation.

Finally, in developing modes of operation one is usually concerned with the sequence in which certain measurements are made rather than the actual hardware equipment required to make the measurements. Consequently, no details will be given here of the equipment to be used. Rather the emphasis will be on the measurement sequence and the methods of combining measurements to determine useful quantities.

For convenience most of the discussion will be in terms of a monostatic system but all of the concepts are appropriate to the bistatic situation. The electromagnetic wave studies at MF and HF will be primarily concerned with transmitting pulses and determining the time delay, amplitude, phase and Doppler shift of any echoes received. As pointed out by Calvert (1976), coherent detection of echoes preserves these signal properties and if the in phase and quadrature components of the coherently detected signal are digitized, further signal processing can be done by a computer or dedicated microprocessors. Details of actual receivers, coherent detectors and AGC circuits will not be given here since such devices are routinely built for communications and radar applications.

2. Amplitude Measurements

After coherent detection, the in-phase and quadrature components of the signal are available for processing. Because of the large range of signal amplitudes which can occur it is unlikely that a detector with sufficient dynamic range could be easily designed. The standard approach is to adjust the receiver gain

using an AGC system so that the input signal to the detector will be at an appropriate level. Thus the measurement of signal amplitude requires the measurement of two quantities, the AGC level (receiver gain) and the output level of the detector. It is unlikely that the AGC will be adjusted more than once for each transmitted pulse and it may be adjusted at a slower rate. To obtain an upper limit on the data rate from the experiment it will be assumed that the AGC level is measured at the rate at which RF pulses are transmitted. For digital processing it is convenient to step the AGC by discrete amounts.

Suppose that for each AGC setting, the output of the AGC is divided linearly into 256 levels so that it can be represented by an 8 bit word. The dynamic range at each gain setting is then 48 db ($20 \log_{10} 256$). If we assume an overall dynamic range of 200 db is required, the AGC control must cover 150 db. If the AGC level is changed when the detector output changes by a factor of $10^{1/8}$, the AGC will have 60 levels which requires 6 bits. The AGC is changed when the maximum signal amplitude changes by the relatively small amount of $10^{1/8}$ (2.5 db) to ensure that most of the full dynamic range of the detector (48 db) is used for each transmitted pulse. By choosing a factor which is a power of 10, the 8 bit words which represent the signal amplitude (the AGC level and the detector output) are easily combined to give the logarithm of the signal amplitude.

3. Phase Measurements

The phase may be obtained from the in-phase and quadrature components of the detected signal. If we present the complex detected signal by $z = x + jy$ where x and y are the in-phase and quadrature components, the phase of the signal is given by

$$\tan \phi = \frac{y}{x}.$$

The error in ϕ, $\delta\phi$ is related to the errors, δx and δy, in x and y, by

$$\delta\phi = \sin\phi \cos\phi \left(\frac{\delta x}{x} + \frac{\delta y}{y}\right).$$

Now for the same error in x and y, (i.e. $\delta x = \delta y$) we have

$$\delta\phi = \sin\phi \cos\phi \left(1 + \frac{x}{y}\right) \frac{\delta x}{x}$$

$$= \sin\phi \, (1 + \cot\phi) \frac{\delta x}{A}$$

$$= (\sin\phi + \cos\phi) \frac{\delta x}{A}$$

where A is the amplitude of the signal. For a given $\delta x/A$, the maximum error in ϕ occurs when $\phi = 45°$

$$\delta\phi_{max} = \frac{\delta x}{A}$$

If the phase is to be measured to within 10°, then $\delta x/A \lesssim .17$. Now the output of the detector is quantized into 256 levels so the quantization error is 1/512 of full scale. This quantization error is therefore less than 17% for all signals with amplitudes greater than 1.2% of full scale of the detector output. Consequently, for the criteria previously outlined for amplitude measurement, the phase of signals can be measured to better than 10° over a dynamic range of 38 db ($-20 \log_{10} .012$) for each AGC setting. Thus the procedure outlined for amplitude measurement also provides acceptable phase measurements.

If a 12 bit word were chosen for each amplitude, then the dynamic range at each gain setting would be 72 db and the phase would be measured to within 10° over a dynamic range of 45 db.

Ground based measurements with an ionosonde have shown that the phase can be consistently measured to within 10° (Devlin et al., 1977). It may be worth noting that Devlin et al. measured the phase more directly, by using limiting detection of echo signals. Such an approach could also be used for the Wave Injection Experiment; the amplitude and phase, however, still require two computer words for their representation. Final choice between the two possible methods of measurement depends on hardware design considerations. Both may be considered "state of the art" techniques and the final choice does not affect the considerations here.

4. Group Path (Apparent Range) Measurements

If pulses of length τ sec. are transmitted, the corresponding receiver bandwidth is $1/\tau$. In order to preserve the signal information after detection, each component of the detected signal must be digitized at a rate of $2/\tau$. If the detector output is continuously digitized at this rate the group path will be measured to within $c\tau/2$. In the monostatic situation, the group path will be twice the apparent range to the echoing region. Hence the resolution in apparent range will be 0.25 $c\tau$. Thus for a bandwidth of 10 kHz, pulses of 15 km in apparent range would be transmitted and the apparent range quantization would be 7.5 km so that the apparent range could be measured to ±3.75 km.

Range Vernier. The above range resolution may be improved by combining measurements made on two adjacent frequencies. The basic definition of group path path, P' is (e.g. Budden, 1961)

$$P' = \frac{\partial}{\partial f}(fP)$$

where P is the phase path at frequency f. Now the phase of an echo signal, ϕ is related to P by

$$\phi = \frac{2\pi f P}{c} .$$

If the phase is measured on two frequencies differing by f, then

$$\frac{\Delta\phi}{\Delta f} = \frac{2\pi}{c} \frac{\Delta(fP)}{\Delta f} = \frac{4\pi}{c} R'$$

where R' is the apparent echo range. Now the measured phase difference can only be between 0 and 2π but the actual phase difference may be greater than 2π.

Thus $\Delta\phi = 2n\pi + \delta\phi$ where n is an integer and $\delta\phi$ is the measured phase difference, and

$$R' = n \frac{1}{2} \frac{c}{\Delta f} + \frac{c}{4\pi} \frac{\delta\phi}{\Delta f} \qquad (4.1)$$

Consequently, only the second term in (4.1) can be determined by the measured phase difference between two frequencies. The maximum value of the second term is $1/2\ c/\Delta f$. If $\Delta f = 20$ kHz, the maximum value is 7.5 km. Since the range can be measured to the nearest 7.5 km by the method outlined previously, the first term in (1) can be determined. If the phase difference can be measured to within $\sim 20^\circ$, equation (4.1) can be used to determine R' to better than 0.5 km.

A comment on approximating the derivative $\partial\phi/\partial f$ by $\Delta\phi/\Delta f$ is appropriate. Assume that the phases ϕ_1, and $\phi_1 + \Delta\phi$ at the frequencies f_1 and $f_1 + \Delta f$, are known. We choose to calculate R' at the frequency, f mid-way between f_1 and $f_1 + \Delta f$.

i.e. $f = f_1 + \Delta f/2 = f_1 + \delta f$.

Then, using Taylor's theorem we may write

$$\phi_1 = \phi(f - \delta f) = \phi_f - \left(\frac{\partial \phi}{\partial f}\right)_{\phi_f} \delta f + \frac{1}{2}\left(\frac{\partial^2 \phi}{\partial f^2}\right)_{\phi_f} (\delta f)^2 - \frac{1}{6}\left(\frac{\partial^3 \phi}{\partial f^3}\right)_{\phi_f} (\delta f)^3 + \ldots .$$

$$\phi_1 + \Delta\phi = \phi(f + \delta f) = \phi_f + \left(\frac{\partial \phi}{\partial f}\right)_{\phi_f} \delta f + \frac{1}{2}\left(\frac{\partial^2 \phi}{\partial f^2}\right)_{\phi_f} (\delta f)^2 + \frac{1}{6}\left(\frac{\partial^3 \phi}{\partial f^3}\right)_{\phi_f} (\delta f)^3 + \ldots$$

$$\therefore \frac{\Delta\phi}{\Delta f} = \left(\frac{\partial \phi}{\partial f}\right)_{\phi_f} + \frac{1}{24}\left(\frac{\partial^3 \phi}{\partial f^3}\right)_{\phi_f} (\Delta f)^2 + \ldots .$$

Now, the error in equating the L.H.S. to the first term on the R.H.S. is

$$\sim \frac{1}{24}\left(\frac{\partial^3 \phi}{\partial f^3}\right)_{\phi_f} (\Delta f)^2 = \frac{\pi}{6c} \frac{\partial^2 R'}{\partial f^2} (\Delta f)^2$$

and this term will generally be quite small.

The discussion of the Range Vernier technique has ignored the phase change between transmitted pulses which occurs due to the satellite motion, (i.e. the Doppler effect) and this point is discussed later in the section on Combined Doppler and Group Delay derived from Phase Measurements.

Range Window. The time between transmitted pulses defines a range window for the apparent range. Echoes arriving from greater apparent ranges will either appear at a shorter range as determined by the time difference between the most recently transmitted pulse and the echo, or will not be detected if the receiver frequency has been changed by more than the bandwidth of the receiver. For the proposed Spacelab orbit, a range window of 500 km is appropriate in most instances. This corresponds to a transmitter pulse repetition rate (prf) of 300 pulses per second (pps). In the equatorial region, long range echoes (up to 5000 km or more) occur as a result of field-aligned propagation along spread F bubbles and other irregularities. Such ranges can be detected umambiguously by

using a p.r.f. of 30 p.p.s. It will be shown later that such a p.r.f. is too low to make the required Doppler measurements. Range ambiguities produced by higher p.r.f.'s can be removed in two ways. Firstly, the Doppler shift may be used since the longer delay echoes will generally have a different Doppler shift than the shorter delay vertical incidence echoes. However, this method requires some knowledge or assumption of the propagation paths involved and may not always reliably remove range window ambiguities. Secondly, coded pulses could be transmitted and the code varied from pulse to pulse and over a sufficient number of pulses so that no ambiguities remain. Each code would require its own detection system. This approach would not add significantly to the hardware of the system, but it would increase the amount of data to be digitized. Each additional pulse code would require an extra in-phase and quadrature amplitude to be digitized. If a p.r.f. of 300 p.p.s. is used and echoes with ranges of, say, up to 3000 km are to be unambiguously measured, six pulse codes would be required.

5. Doppler Measurements

One standard method of Doppler measurement is to pass the detected signal through a series of narrow band filters, the output of which correspond to the Doppler spectrum of the signal. While this method gives the instantaneous Doppler directly, there are two distinct disadvantages. The first is that the amount of data to be digitized is proportional to the number of filters and hence will increase rapidly if good Doppler resolution is required. The second is that the filter characteristics need to change with the transmitted frequency and this would complicate any hardware approach. (The reasons for requiring the filter characteristics to change with frequency will be apparent later).

An alternative approach is to measure the phase of an echo signal as a function of time and to calculate the Doppler spectrum using the Fast Fourier Transform (FFT). This method has two main advantages. Firstly, it uses the phase information already available from the echo amplitude measurements and so does not increase either the hardware required or the number of measurements to be made. Secondly, at a given transmitter frequency, the frequency range and resolution of the Doppler spectra will be determined by the transmitter prf and the total time for which measurements are made. These parameters may be readily changed by software in the computer control system and so the required changes in Doppler resolution as the transmitted frequency changes can be more easily made.

It may seem a disadvantage that this method combines measurements over some period of time and does not give an instantaneous Doppler as is obtained with hardware filter circuits. However, such filter circuits involve time constants, etc., and some signal integration is required to obtain appropriate frequency resolution and consequently the "instantaneous" values obtained are not based exclusively on the signal components received at a given time.

Interpretation of Doppler

The general formula for the Doppler shift in a refractive medium, is given by (Bennett, 1968)

$$\Delta f = -\frac{f}{c}\left\{\int_A^B \frac{\partial \mu}{\partial t}\cos\alpha\, ds + [\underline{p}\cdot\underline{v}]_A^B\right\} \qquad (5.1)$$

where μ is the refractive index

$\underline{p}$ is a vector in the direction of the wave normal with magnitude, μ,

$\underline{v}$ is the vector velocity of a point on the ray

A and B are the end points of the ray.

Consider initially an ionosphere which is plane stratified (but not necessarily in the horizontal plane) and which is not varying with time. For an orbiting experiment, the Doppler effect will be due to the relative motion of the orbiting vehicle and the ionosphere. For rays reflected back to the vehicle in the usual way (Figure 1), the Doppler shift is given by (e.g. Dyson, 1975)

$$\Delta f = \frac{2f}{c} \underline{p}_A \cdot \underline{v} \tag{5.2}$$

$$= \frac{2f}{c} \mu_A v \cos\theta \tag{5.3}$$

where μ_A is the refractive index at the vehicle, $\underline{v}$ is the vehicle velocity and the angle between the wave normal direction and the vehicle velocity.

If the reflection point is not at the $\mu = 0$ level, but is due to an irregularity at some other level, several return paths are possible (Figure 2).

For paths 1 and 2 in Figure 2, the Doppler shift is still due entirely to the motion of the end point A and (5.2) still applies and can be used to obtain θ_1 and θ_2. For rays outgoing along 1 and returning along 2, or vice versa,

$$\Delta f = \frac{f}{c} (\underline{p}_{A_1} + \underline{p}_{A_2}) \cdot \underline{v} \tag{5.4}$$

$$= \frac{f}{c} (\mu_{A_1} \cos\theta_1 + \mu_{A_2} \cos\theta_2) \tag{5.5}$$

and so equals the average Doppler shift for the signals returned by ray paths 1 and 2. If the ionosphere has a velocity $\underline{v}_I$, then $\underline{v}$ must be replaced by $\underline{v} - \underline{v}_I$ in (5.2) and (5.3). However, the corrections will generally be minor since $|\underline{v}| >> |\underline{v}_I|$.

For the more general case in which the background ionosphere is not horizontally stratified, equations (5.2) and (5.3) still apply if $\partial\mu/\partial t$ is approximately constant along the ray path (Dyson, 1975) and this situation is likely to hold for large scale features, such as TID's, which produce refractive effects.

Hence, monostatic measurements of Doppler shift from an orbiting vehicle may be regarded as measurements of angle of arrival provided the refractive index at the satellite and the vehicle velocity are known. The earth's magnetic field causes the refractive index to depend on the wave normal direction and also causes the ray direction to differ from the wave normal direction. These relationships are well known and may be accounted for. In many cases, however, these complications may be neglected provided the frequencies under consideration are not near the frequencies reflected at the orbiting vehicle. The plasma frequency and gyrofrequency at the vehicle are measured by the WIF and may be considered sufficient information to determine μ_A.

The ability to measure angle of arrival is very important. It will enable the nature of ionospheric structures to be determined more precisely. An obvious example is ducted field aligned propagation which occurs generally near the magnetic equator (Muldrew, 1963) and can occur in association with equatorial plasma bubbles (Dyson and Benson, 1978). Angle of arrival information would give confirmation that the propagation is in fact field-aligned and would allow the trapping mechanism to be studied in more detail. The question of whether extra traces usually attributed to conjugate ducting are always due to ducting or are sometimes due to simple refraction (Lobb and Titheridge, 1977) would also be resolved.

Equation (5.2) may be re-written as

$$\frac{\Delta f}{f} = \frac{2}{c} \mu_A \, v \cos \theta .$$

Assuming a vehicle velocity of 8 km/sec, and $\mu_A \approx 1$ for frequencies greater than 1.5 times the plasma frequency at the vehicle, a Doppler resolution $\Delta f/f$ of 0.6×10^{-6} gives an angular resolution about $\theta = 0°$ of $\sim 10°$. Near $\theta = 90°$ (vertical incidence) the angular resolution is $\sim 1°$. This resolution in Doppler corresponds to a change in Doppler of 1.8 Hz at 3 MHz and 6 Hz at 10 MHz. To achieve these resolutions measurements would have to be made for at least 0.56 seconds at 3 MHz and 0.17 seconds at 10 MHz.

The FFT method will be used to calculate the Doppler from the phase measurements vs. time. The highest Doppler shifts will be of the order of 150 Hz at 3 MHz and 550 Hz at 10 MHz. To prevent aliasing, the phase must be measured at a rate of 300 samples per second at 3 MHz and 1100 samples per second at 10 MHz. As discussed earlier, a p.r.f. of 300 provides an appropriate range window (500 km), but the smaller range window associated with significantly higher p.r.f.'s will be generally unacceptable. It is possible to use lower p.r.f.'s and remove the Doppler aliasing by transmitting first at one p.r.f. and then at another. For example, suppose a measured sequence is made at a particular p.r.f. There will be an ambiguity for a Doppler frequency greater than half the p.r.f. If a second measurement sequence is obtained at a p.r.f. of 0.67 of the first p.r.f., the ambiguity can be removed since the ambiguous frequencies of the first spectra will appear as distinguishable apparent frequencies in the second spectra.

Suppose that the aliasing frequency for the first p.r.f. is f_a. An apparent frequency f_{x1} may be any frequency f which satisfies the relation $f = 2nf_a \pm f_{x1}$, $n = 0, 1, 2, \ldots$ For the second p.r.f., the relationship may be written $f = 2n(.67)f_a \pm f_{x2}$, $n = 0, 1, 2, \ldots$ It is apparent that for a given f, $f_{x1} = f_{x2}$ only when $n = 0$. If a Doppler frequency f produces spectral peaks at f_{x1} and f_{x2} in the two spectra, then

$$2nf_a \pm f_{x1} = 2n\,(0.67)\,f_a \pm f_{x2}$$

and

$$n = \frac{f_{x2} \mp f_{x1}}{0.66\ f_a}\ .$$

For example, suppose a peak occurs at $0.50\ f_a$ in the first spectra and at $0.16\ f_a$ in the second,

$$n = \frac{-0.34}{0.66} \text{ or } 1$$

Since n must be a positive integer, $n = 1$ and $f = 1.5\ f_a$. If the higher p.r.f. is chosen to be 300 p.p.s., then for frequencies up to 10 MHz, $n \leq 4$. Of course if many peaks occur in the spectra some ambiguity in interpretation may remain.

Simple Doppler Measurement

If two consecutive pulses are transmitted on the same frequency and the phase difference measured, the Doppler shift may be calculated directly. This will give a reliable Doppler measurement for discrete echoes with a large signal to noise ratio. When noise is present the method may still be used by transmitting several pulses and determining the average Doppler shift. When more than one echo is present at the same apparent range this method will give some weighted average depending on the amplitudes and Doppler shifts of the individual

echoes. In this case the full Doppler spectrum must be measured in order to resolve the echoes. However, if one echo has significantly greater amplitude than other echoes the simple Doppler measurement will be a reasonable approximation. The simple Doppler measurement will be a very useful technique because well defined discrete echo traces often occur and the technique is ideally suited for use with a swept frequency mode of operation.

The Doppler shift and phase are related through the following expressions ($\mu \approx 1$):

$$\Delta f = \frac{2f}{c} v_{sat} \cos\theta = \frac{f}{c} \frac{dP}{dt}$$

$$\phi = 2\pi f P/c.$$

Now

$$\frac{\Delta\phi}{\Delta t} = \frac{2\pi f}{c} \frac{\Delta P}{\Delta t} = \frac{4\pi f}{c} v_{sat} \cos\theta$$

Now, for a p.r.f. of 300 p.p.s., and a vehicle velocity of 8 km/sec, the phase change between pulses is

$$\Delta\phi \simeq .36 \times 10^{-6} f \cos\theta.$$

The measured phase difference will be in the range of $\pm\pi$, so that

$$\Delta\phi = 2n\pi + \delta\phi$$

where $\delta\phi$ is the measured phase between $\pm\pi$. Consequently, the angle of arrival may be aliased. The maximum apparent angle, θ_m will be given by

$$|\cos\theta_m| = \frac{10^7}{3.6f} = 1 \quad \text{for} \quad f \geq 2.8 \text{ MHz}.$$

Thus there will be no aliasing in the angle of arrival for frequencies less than 3 MHz. (This result is expected in view of the discussion in the previous section). At 10 MHz, $|\cos\theta_m| = 1/3.6$ and $\theta_m = 74°$ so that $90° \leq \theta_{apparent} \leq 74°$.

For discrete echo traces, the apparent angle of arrival will vary as a function of the transmitter frequency in a predictable way enabling ambiguities to be removed.

If the phase difference can be measured to within 20°, the resolution in angle of arrival, $\delta\theta$, will be given by

$$|\cos \delta\theta| = 3.4 \times 10^5 / .36\ f$$

$$\sim 0.1 \text{ at } 10 \text{ MHz}$$

This corresponds to ~6° at $\theta = 90°$ (vertical incidence) and ~16° about $\theta = 0$. At higher frequencies the resolution increases but aliasing becomes more of a problem. Figure 3 shows the variation of $\Delta\phi$ with frequency and angle of arrival for a p.r.f. of 300 p.p.s.

In Figure 4 a situation is shown which can occur near the equator. The Spacelab is in the topside ionosphere and is within a field-aligned duct which produces conjugate ducting. Vertical incidence echoes are also present, as well as backscattering echoes from a patch of field-aligned irregularities below the vehicle. The echo patterns which would be detected using a large range window are shown. In Figure 5 the type of record obtained with a 500 km range window is shown. The echo intensity has been coded with the simple Doppler measurements (i.e. $\Delta\phi$) [in the manner first used by Findlay (1951)], to produce a fringe pattern in each of the discrete echoes. (Because $\Delta\phi$ changes slowly with frequency [as seen in Figure 3], it has been multiplied by about 5 to produce the fringe pattern shown). The vertical incidence echo and the L+S ducted echo (see Figure 4), have zero Doppler shift and the fringes are parallel to the echo contour. The S and 2S+L ducted echoes have a positive Doppler and the fringes move upward as a function of frequency with respect to the echo contour. For

the L ducted echo, the Doppler is negative and so the fringes slope downward. The backscattering from the spread F patch will generally consist of overlapping echoes and coherent echo traces will be difficult to distinguish. However, the closest range edge of the spread F echo patch will correspond to echoes from the edge of the spread F irregularity region and may show fringes of negative slope corresponding to propagation perpendicular to the magnetic field direction.

Combined Doppler and Group Delay Derived from Phase Measurements

In a previous section it was pointed out that a range vernier technique could be used by measuring the phase difference on two frequencies. Since these phase measurements would be made sequentially, the phase difference would include a Doppler shift contribution. This contribution may be removed by transmitting a sequence of three pulses, the first two on one frequency to measure the Doppler and the third at the second frequency, for the range vernier technique.

We may write:

$$\frac{d\phi}{dt} = \frac{\partial\phi}{\partial t} + \frac{\partial\phi}{\partial f}\frac{df}{dt}$$

where $d\phi/dt$ is the measured rate of change of phase between two consecutive pulses, $\partial\phi/\partial t$ is the Doppler contribution, df/dt is the sweep rate of the transmitter, and $\partial\phi/\partial f$ is the contribution associated with the path of propagation. If ϕ_{11}, ϕ_{12}, and ϕ_{21} are the measured phases of the three consecutive pulses transmitted at intervals of Δt and at frequencies f_1, f_1 and $f_1 + \Delta f$, respectively, then

$$\left(\frac{d\phi}{dt}\right)_1 = \frac{\partial\phi}{\partial t} \simeq \frac{\phi_{12} - \phi_{11} + 2n\pi}{\Delta t}$$

and

$$\left(\frac{d\phi}{dt}\right)_2 = \frac{\partial\phi}{\partial t} + \frac{\partial\phi}{\partial f}\,\frac{df}{dt} \simeq \frac{\phi_{21} - \phi_{12} + 2m\pi}{\Delta t}$$

Hence

$$\frac{\partial\phi}{\partial f} \cdot \frac{df}{dt} = \left(\frac{d\phi}{dt}\right)_2 - \left(\frac{d\phi}{dt}\right)_1$$

$$= \frac{\phi_{21} - 2\phi_{12} + \phi_{11} + 2(m-n)\pi}{\Delta t}$$

$$\therefore \frac{\partial\phi}{\partial f} \simeq \frac{\phi_{21} - 2\phi_{12} + \phi_{11} + 2(m-n)\pi}{\Delta f}$$

Hence both $\partial\phi/\partial t$ and $\partial\phi/\partial f$ may be determined with the usual $2n\pi$ ambiguity, the effect of which has already been discussed.

Since three phase measurements are involved the errors will be greater than before, but with the values adopted in the section on "Range Vernier" the apparent range would be determined to within 1 km.

6. Pulse Synthesis

Although the Range Vernier technique allows the group path to be readily measured to within 1 km, the ability to separate closely spaced echoes is determined by the length of the transmitted pulse, assumed here to be 15 km. If better resolution of echoes is required, pulse compression techniques must be used if the receiver bandwidth is not increased. One simple method has been used successfully with ground based ionosondes (Hammer and Bourne, 1976; Devlin et al., 1977). The ionosonde is operated in the usual way in that a sequence of pulses is transmitted consecutively over an appropriately limited frequency range. The amplitude and phase of any echoes are measured. The echoes associated with a particular echo trace (e.g. one hop vertical incidence F-region echoes)

may then be regarded as the "frequency components" of an echo signal due to a synthesized pulse whose frequency spectrum is the sequence of transmitted pulses. The delayed synthesized echo is then obtained by Fourier transformation of the amplitude and phase of the "frequency components." Quite narrow pulses can be synthesized and echoes separated by 1 km in range readily resolved (Devlin et al., 1977). The method is discussed in detail by Devlin et al. (1977). It is an indirect form of pulse synthesis but is discussed here because, for the type of computer controlled system envisaged, its implementation depends only on appropriate software. It could also conceivably be used in later analysis of certain swept frequency modes of operation not specifically designed with this technique in mind. If pulse synthesis is required as a primary operation mode, however, more conventional methods should probably be used since the technique described here is relatively time consuming both from the point of view of measurement time and the amount of analysis required to obtain good echo resolution.

7. Location of Echoing Regions

Vertical incidence echo traces may be inverted to obtain the electron density distribution with height. The procedures may also be applied at other angles of incidence and this has been done by Dyson and Benson (1978), for example, to determine the electron density distribution along magnetic field-aligned bubbles. In the absence of angle of arrival measurements, this type of analysis is usually not attempted when it is obvious that the angle of arrival is changing significantly with frequency, e.g. when TID's cause echo traces which exhibit "kinks" or splitting. Angle of arrival information will be available in the Spacelab experiment and such techniques, combined with ray tracing, will enable echo traces to be inverted to obtain the irregularity structure.

An approximate method of locating irregularity regions distant from Spacelab will be discussed in the section on Fixed Frequency operation

8. Operation Modes

Swept Frequency Mode. This mode will be a basic exploratory mode aimed at getting a reasonably complete picture of the ionosphere in a short time. Thus both range and angle of arrival (Doppler) information are required, the latter being obtained by the Simple Doppler Method. The principles of operation will be those outlined in section 5, i.e., a group of three pulses, two at the same frequency f and a third at a slightly higher frequency, $f + \Delta f$. A frequency interval Δf of 20 kHz will give ranges within 1 km using the Range Vernier technique.

Suppose 3 sets of pulses (i.e. a total of nine pulses) are transmitted to improve operation in the presence of noise, and that f is then increased by 25 kHz if below 1 MHz and by 100 kHz if above 1 MHz. If a p.r.f. of 300 p.p.s. is used, the frequency range from 500 kHz to 30 MHz will be swept in 4.5 seconds. Generally, ionospheric echoes will occur over a much smaller frequency range than this and it will not be necessary to cover the whole range of 500 kHz to 30 MHz. Consequently, very rapid soundings can be made and the resolution of the measurements along the orbital path would be better than 35 km. Above 1 MHz, range measurements at every 100 kHz in frequency are sufficient for calculating the electron density distribution by inversion techniques.

"Fixed Frequency" Measurements. In this mode measurements are made at a small number of frequencies, say up to 10. This mode can be considered to be a variation of the previous mode since a certain frequency range must be cycled through using discrete steps. If the same form of transmission is used as for the Swept Frequency Mode (i.e. three sets of three pulses, prf of 300 pps),

10 frequencies would be cycle through in 0.3 seconds giving a resolution along the orbit of a few kilometers. This mode will be particularly useful for studying various types of ionospheric structure such as TID's, patches of spread F distant from Spacelab and bubble structures of small transverse dimensions.

Figure 6 shows a Doppler coded group delay vs. time record produced by an irregularity displaced from the orbital path. At closest approach, the Doppler shift is zero and the group delay a minimum.

Depending on the number of frequencies being cycled inrough, and their spacing, it may be possible to invert the vertical incidence data and determine the electron density contours of the background ionosphere. Ray tracing could then be used to determine the location of the irregularity shown in Figure 6.

Alternatively, the location may be estimated as follows. If the earth's magnetic field is neglected, the group range of an oblique echo may be related to the group height at vertical incidence, by (Calvert and Cohen, 1961),

$$h_R'^2 = h_v'^2 + R^2 \tag{8.1}$$

$$h_v'/f_v = h_R'/f_R \tag{8.2}$$

where R is the horizontal range to the irregularity, h_R' is the apparent range at the frequency f_R, and h_v' is the apparent vertical range at f_v, the frequency reflected vertically at the same height as the oblique ray at frequency f_R, (see Figure 7). Now according to Martyn's Theorem

$$f_v = f_R \cos\theta \tag{8.3}$$

where θ_o is the angle of incidence at the $\mu = 1$ level.

For a vehicle imbedded in the ionosphere, Snell's Law gives

$$\mu_{sat} \cos\theta_{sat} = \sin\theta_o \tag{8.4}$$

If the vehicle is moving horizontally with velocity v, at an angle of ψ to the plane containing the ray path (Fig. 8), the Doppler shift may be written as

$$f = \frac{2f}{c} \mu_{sat} \, v \sin \theta_{sat} \cos \psi \tag{8.5}$$

Using (8.1), (8.2) and (8.3) gives

$$h'_R \sin \theta_o = R \tag{8.6}$$

Using (8.6), (8.4) and (7.5) we obtain

$$R \cos \psi = \frac{2\Delta f}{f} \frac{c}{v} h'_R \tag{8.7}$$

Hence, measurements of apparent range h'_R and Doppler shift Δf enable the projection of the irregularity true range along the vehicle orbit to be obtained. Consequently, the location of irregularities can be estimated from portions of Fixed Frequency records, or even Swept Frequency records. That is, it is not necessary to observe either a crossing of zero Doppler shift or a minimum in apparent range in order to determine the position of the irregularity.

Doppler Spectra. This mode requires operation at one frequency for ~0.6 seconds. It is consequently a relatively time-consuming mode of operation. It is best used by alternating with swept frequency modes or interspersing it at fixed time intervals in the Fixed Frequency Mode. Five or ten selected frequencies could be used taking approximately a total time of 2.5 or 5 seconds to obtain the Doppler Spectra.

A future development to consider is one in which two receivers are used, one for Doppler spectra and the other for the Swept Frequency and Fixed Frequency Modes. A second transmitter would not be needed, since the transmitter would only need to be capable of transmitting two interlaced sequences of pulses with a sufficient frequency difference so that each receiver would only be sensitive to one or other of the sequences.

Control Program. The operation mode of the instrument and selection of operating parameters (frequency, p.r.f., step size, etc.) will be under computer control. The operation modes will be selected or changed by providing the appropriate input parameters to the control program. The appropriate input for several types of operation sequences will be available from the computer memory. The payload specialist will be able to enter other operation sequences. It is reasonably straightforward to program several modes of operation and allow a wide choice of parameters (e.g. sequence of modes, swept frequency range, frequency step, number of fixed frequencies, etc.) and this approach has been used successfully with ground based ionosondes (e.g. Devlin, 1978).

9. Data Rates

In the discussion, thus far, all techniques have been based on measurements of the in-phase and quadrature amplitude compoents of the signal. In section 3, a 10 kHz bandwidth was assumed so that the in-phase and quadrature amplitudes need to be sampled at a 20 kHz rate. Each amplitude is assigned either an 8-bit or 12 bit word, so that the measurements require a data rate of 40 k words/sec.

The maximum p.r.f. suggested here is 300 p.p.s. and for each pulse the frequency and AGC level must be recorded. The AGC requires one word or less (see Section 2). In the MF and HF range, frequency steps as small as 20 kHz have been used in this discussion. It is unlikely that other modes of operation would require a frequency step of less than 1 kHz. If the frequency is to be specified to 1 kHz, we can divide each range of 1 megahertz into 4 sub-ranges of 250 kHz. The basic range of 250 kHz can be specified by 8 bits, and to determine the correct sub-range over 30 MHz requires 7 bits. Thus two words are required to specify the frequency.

Hence, the overall word rate is 40.9 k words/sec. A rate of 41 k words/sec. would allow 100 words/sec for other information, such as universal time, and operating mode to be specified periodically. For 8 bit words, this corresponds to a bit rate of 3.28×10^5 bits/sec.

10. Oblique Measurements

The types of measurements discussed previously can all be done by transmitting from one vehicle and receiving on another. Some advantages of doing this have been discussed by Calvert (1976) and will not be repeated here. Only one aspect of combining Doppler and time delay measurements between two vehicles will be discussed.

From measurements on a single vehicle, the apparent range and angle of arrival (as deduced from the Doppler shift) can be determined. The apparent range, R' defines a sphere in R' space on which the echo lies. Since echoes returning from in front of the vehicle have a Doppler shift of different sign to those returning from behind the vehicle, the angle of arrival defines a circle on the sphere on which the echoing region must lie (Figure 9). In the absence of further measurements, more precise location of the echoes requires assumptions to be made and in some instances these may be reasonable. For example, if the angle of arrival corresponds to propagation along the magnetic field direction, it would be entirely reasonable to assume that propagation was along the field line rather than at an angle to it. In other situations, however, it is likely that simplifying assumptions could not be made with confidence.

If measurements are made between two vehicles, then the apparent time delay, which is equivalent to an apparent path length, P' defines an ellipsoid upon which the echoing region must lie (Figure 10). Since the echoing region can

be confined to a circle by the single vehicle measurements, then, in the case of point-like echoing regions, the echoing region must lie on the intersection of the circle with the ellipsoid. The cross section of the ellipsoid in the plane containing the circle will be an ellipse. The ellipse and the circle can have from 2 to 4 intersections (Figure 11). When there are 3 or 4 intersections, some of the ambiguity may be reduced by using the Doppler shift information for propagation between the two satellites as follows. Since the apparent range from the vehicle containing the monostatic measurements is known, the apparent range from the other vehicle is just the difference between the monostatic range and the apparent path length between the vehicles. In this way the location of the echoing region is either determined uniquely or known to be one of two possible locations. With the geometry of the situation now known, the expected Doppler shift between the two vehicles can be calculated and the degree of agreement with the measured Doppler shift will indicate the extent to which the reflecting region acts like a point reflector. If there is significant disagreement, some knowledge of the extent of the reflecting surface may be estimated by considering different models.

11. Measurements of the Horizontal Wave Vector of Gravity Waves

Combining Monostatic H.F and Bistatic VHF Measurements

Suppose Spacelab contains the H.F. monostatic system and that the subsatellite has a VHF receiver to measure the Doppler of a VHF signal transmitted from Spacelab. For simplicity it is assumed that the two vehicles are traveling northward and separated by a distance L in the east-west direction (Fig. 12). Both vehicles travel horizontally and with the same velocity.

Suppose that there is a wave-like perturbation in the electron density and that in the horizontal plane containing the space vehicles the variation in electron density can be written as

$$\Delta N(x,y) = \Delta N_0 \cos 2\pi \left(\frac{x}{\lambda_x} - \frac{y}{\lambda_y} \right) \tag{11.1}$$

i.e. wavelike perturbation with apparent wavelengths λ_x in the x direction and λ_y in the y direction (Fig. 12). Fronts of constant phase occur where $y = (\lambda_y/\lambda_x)x$ i.e. phase fronts are tilted to the x axis at an angle $\theta = \text{artan } \lambda_y/\lambda_x$ and the wave vector is at an angle $\pi/2 - \theta$ to the x axis and the true wavelength λ_T is given by $1/\lambda_T^2 = 1/\lambda_x^2 = 1/\lambda_y^2$. Spacelab moves along the line $x = 0$.

The variation in N_e along the orbit of Spacelab is of the form

$$\Delta N_s = \Delta N_0 \cos 2\pi \left(- \frac{y}{\lambda_y} \right)$$

$$= \Delta N_0 \cos 2\pi \left(- \frac{vt}{\lambda_y} \right) \tag{11.2}$$

and so λ_y can be determined.

The sub-satellite moves along the line $x = L$. Consider the phase path P, of a VHF ray propagating from Spacelab to the sub-satellite.

$$P = \int_{ray} \mu \cos \alpha \, ds$$

For VHF we may consider ray paths to be line of sight, so that

$$P = \int_0^L \mu dx$$

Ignoring the magnetic field (again an excellent approximation at VHF),

$$\mu^2 = 1 - X$$

and

$$\mu \simeq 1 - \frac{1}{2} X \text{ since } X << 1$$

$$= 1 - \frac{1}{2} K \frac{N_e}{f^2} \text{ since } X = \frac{K N_e}{f^2}$$

Thus

$$P = L - \frac{1}{2} \frac{K}{f^2} \int_0^L N_e \, dx$$

$$\frac{dP}{dt} = - \frac{1}{2} \frac{K}{f^2} \frac{d}{dt} \int_0^L N_e \, dx$$

where K is a constant. The Doppler shift is given by

$$\Delta f = - \frac{f}{c} \frac{dP}{dt}$$

$$= - \frac{1}{2} \frac{K}{f^2 c} \frac{d}{dt} \int_0^L N_e \, dx$$

(Note that dL/dt has been assumed to be zero, i.e. we have assumed that the two vehicles maintain their spacing with time. If this is not true then

$$\frac{dP}{dt} = \frac{dL}{dt} - \frac{1}{2} \frac{K}{f^2} \frac{d}{dt} \int_0^L N_e \, dx$$

However if two frequencies are used, as in the proposed experiment (e.g. Grossi and Gay, 1975) we have

$$\frac{dP_1}{dt} = \frac{dL}{dt} - \frac{1}{2} \frac{K}{f_1^2} \frac{d}{dt} \int_0^L N_e \, dx$$

and

$$\frac{dP_2}{dt} = \frac{dL}{dt} - \frac{1}{2} \frac{K}{f_2^2} \frac{d}{dt} \int_0^L N_e \, dx$$

and

$$\frac{dP_1}{dt} - \frac{dP_2}{dt} = -\frac{1}{2} K \left(\frac{f_2^2 - f_1^2}{f_1^2 f_2^2} \right) \frac{d}{dt} \int_0^L N_e \, dx$$

Thus the differential Doppler shift can be used to eliminate dL/dt. Even with measurements on only one frequency, dL/dt is likely to be a slow variation compared with the effect of a gravity wave and so could be filtered out). Thus we are concerned with determining

$$\frac{d}{dt} \int_0^L N_e \, dx$$

Now $N_e = N_{background} + \Delta N(x,y)$. Consider a particular instant when Spacelab is at (o,y) and sub-satellite is at (x,y). The instantaneous value of $\int N_e \, dx$ will be given by

$$N_T = \int_0^L \left(N_b + \Delta N_0 \cos 2\pi \left(\frac{x}{\lambda_x} - \frac{y}{\lambda_y} \right) dx \right.$$

$$= N_b \cdot L + \frac{\lambda_x}{2\pi} \Delta N_0 \left\{ \sin 2\pi \left(\frac{L}{\lambda_x} - \frac{y}{\lambda_y} \right) - \sin 2\pi \left(- \frac{y}{\lambda_y} \right) \right\}$$

Now $y = vt$, so N_T will vary with time according to

$$N_T = N_b \cdot L + \frac{\lambda_x}{2\pi} \Delta N_0 \left\{ \sin 2\pi \left(\frac{L}{\lambda_x} - \frac{vt}{\lambda_y} \right) - \sin 2\pi \left(- \frac{vt}{\lambda_y} \right) \right\}$$

and

$$\frac{dN_T}{dt} = -v \frac{\lambda_x}{\lambda_y} \Delta N_0 \left\{ \cos 2\pi \left(\frac{L}{\lambda_x} - \frac{vt}{\lambda_y} \right) - \cos 2\pi \left(- \frac{vt}{\lambda_y} \right) \right\} \qquad (11.3)$$

which may be written as

$$\frac{dN_T}{dt} = 2v \frac{\lambda_x}{\lambda_y} \Delta N_0 \sin 2\pi \left(\frac{L}{2\lambda_x} - \frac{vt}{\lambda_y} \right) \sin \frac{\pi L}{\lambda_x} \qquad (11.4)$$

Comparing (11.2) and (11.4) we see that the VHF Doppler variation will have the same period as ΔN_s but there is a phase shift of $\pi L/\lambda_x$. Thus if L is known, we can determine λ_x and hence λ_T. (Note however there will be an ambiguity in $\hat{\underline{k}}$, i.e. two possible directions differing by 180°).

From (11.4) we see that if $\lambda_y \to \infty$, there is no dN_T/dt due to the wave. This is the expected result. When $\lambda_x \to \infty$, the phase shift approaches 90° as we expect and since

$$\sin(\pi L/\lambda_x)/(\pi L/\lambda_x) \to 1$$

$$\frac{dN_T}{dt} \to \frac{vL}{\lambda_y}\Delta N_0 \sin 2\pi\left(-\frac{vt}{\lambda_y}\right)$$

i.e. dN_T/dt depends only on λ_y as we expect. Suppose a monostatic HF system or a direct measurement probe is on the sub-satellite. It would measure variations given by

$$\Delta N = \Delta N_0 \cos 2\pi\left(\frac{L}{\lambda_x} - \frac{vt}{\lambda_y}\right)$$

i.e. a phase shift of $2\pi L/\lambda_x$ compared with Spacelab measurement. However, there are ambiguities in λ_x such that

$$2\pi L/\lambda_x = 2n\pi, \quad n = 1, 2, - - -$$

$$\text{i.e., } L/\lambda_x = n\lambda_x$$

In the case of the VHF Doppler experiment there are ambiguities in phase when

$$\pi L/\lambda_x = 2n\pi$$

$$\text{i.e., } L = 2n\lambda_x$$

However, the amplitude term is proportional to λ_x and so the ambiguities can be removed.

Note: The Doppler experiment has zero amplitude when $L = n\lambda_x$ so that the best results would be obtained by combining the VHF Doppler with a local measurement (either by H.F. system or probe) or sub-satellite.

Acknowledgments

This author has been supported by a NAS/NRC Senior Resident Research Associateship at the NASA/Goddard Space Flight Center while on leave from La Trobe University, Australia.

Many stimulating discussions with R. F. Benson, W. Calvert and S. Gross contributed to this work.

References

Bennett, J. A. (1968), Aust. J. Phys., 21, 259

Bibl, K., and B. W. Reinisch (1978), Radio Science, 13, 519.

Budden, K. G. (1961), Radio Waves in the Ionosphere, Cambridge University Press

Calvert, W. (1976), Shuttle Wave Experiments, NASA Report Contract NAS5-23346

Calvert, W., and R. Cohen (1961), J. Geophys. Res., 66, 3125

Devlin, J. C., P. L. Dyson and P. R. Hammer (1977), Radio Science, 12, 767

Devlin, J. C. (1978), Ph.D. Thesis, La Trobe University Australia

Dyson, P. L. (1975), J. Atmos. Terr. Phys., 37, 1151

Dyson, P. L., and R. F. Benson (1978), Geophys. Res. Let., 5, 795

Findlay, J. W. (1951), J. Atmos. Terr. Phys., 1, 353

Grossi, M. D. and R. H. Gay (1975), Smithsonian Astrophysical Observatory Special Report No. 366

Hammer, P. R. and I. A. Bourne (1976), J. Atmos. Terr. Phys., 38, 935

Lobb, R. J. and J. E. Titheridge (1977), J. Atmos. Terr. Phys., 39, 129

Muldrew, D. B. (1963), J. Geophys. Res., 68, 5355

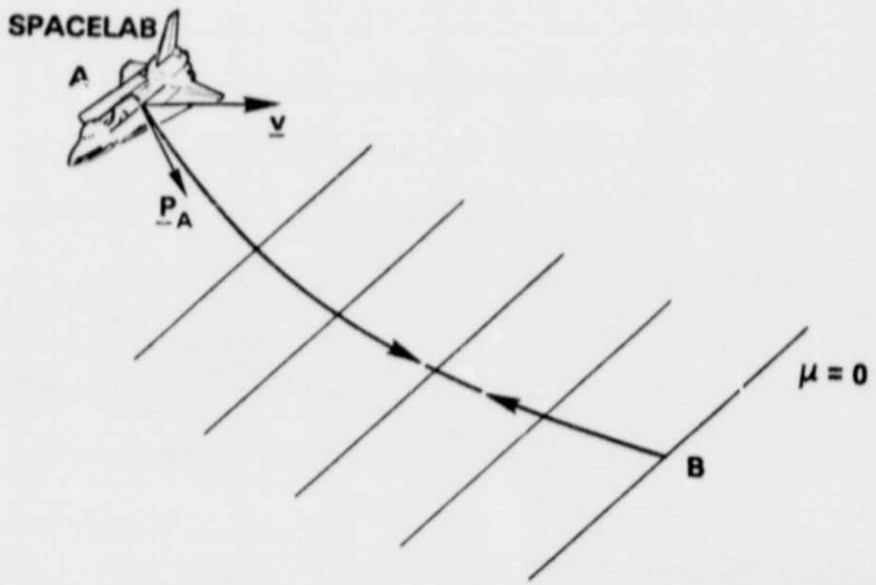

Figure 1. Reflected ray path in a plane stratified ionosphere

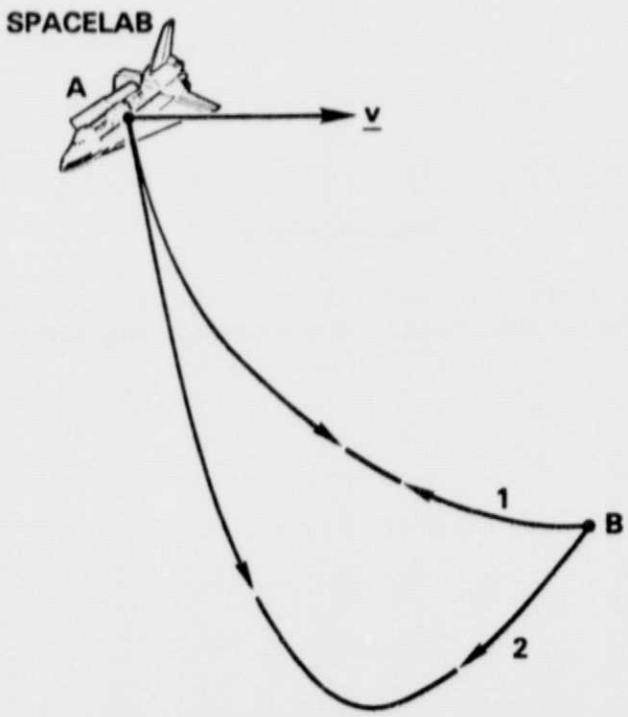

Figure 2. Reflected ray paths from an irregularity embedded in a plane stratified ionosphere

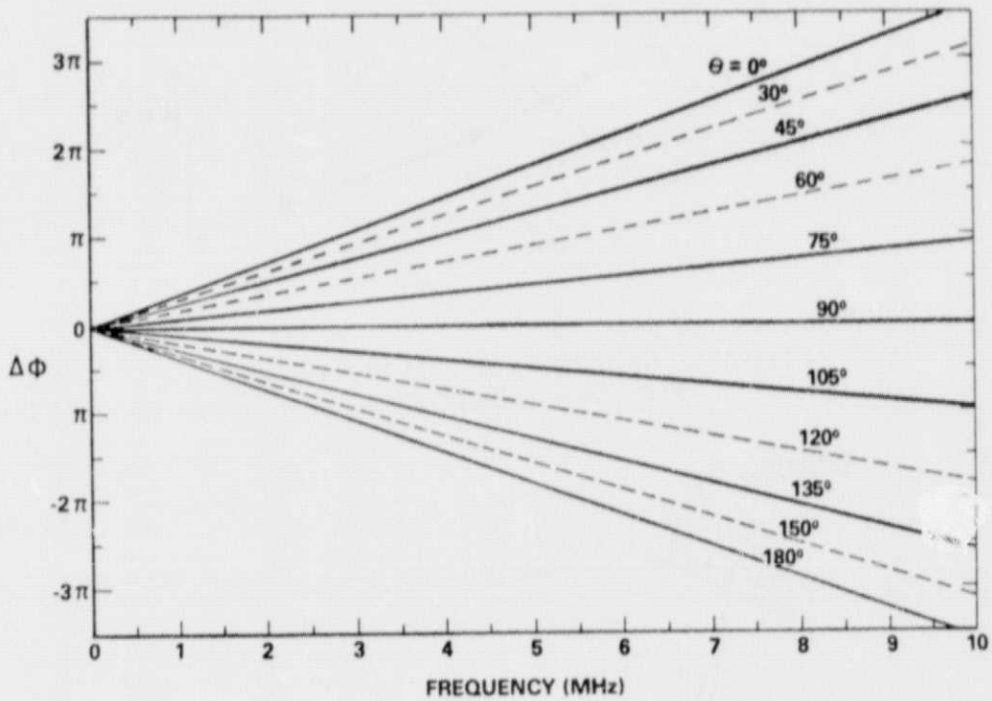

Figure 3. Phase shift due to Doppler effect, $\Delta\phi$, between two echoes of two pulses transmitted at the same frequency but at a time interval of 1/300 sec.

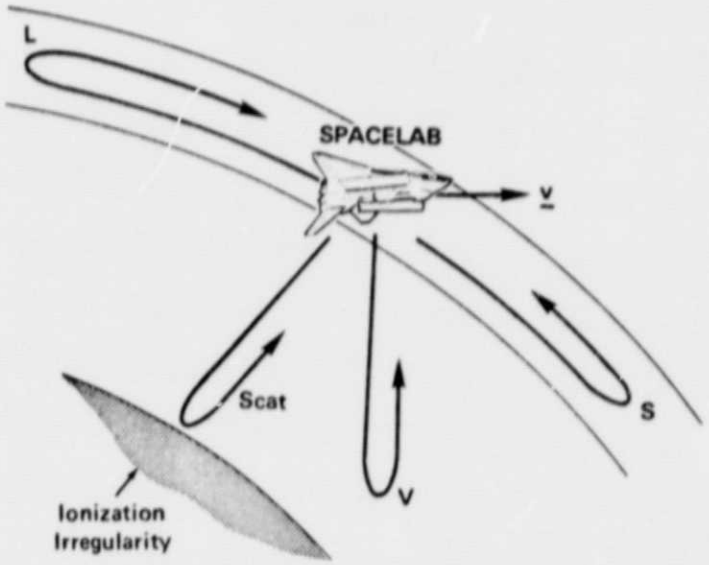

Figure 4(a). Possible echo paths when Spacelab is within an equatorial bubble or duct and when a field-aligned irregularity patch exists below Spacelab

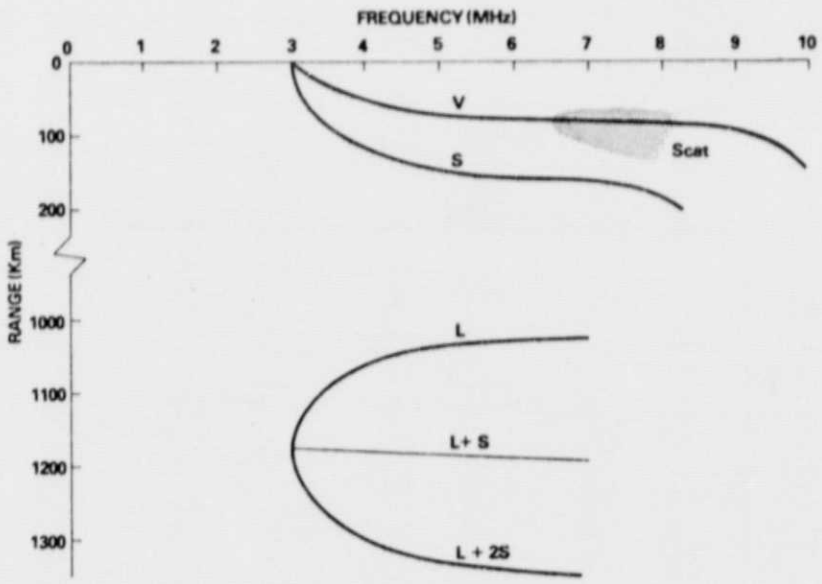

Figure 4(b). Ionogram obtained for the situation shown in Figure 4(a)

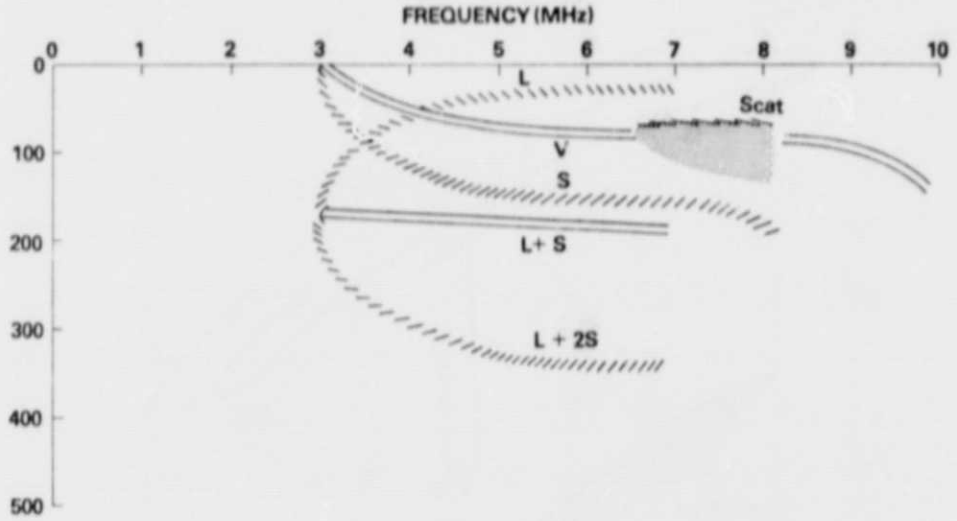

Figure 5. Doppler coded ionogram with a range window of 500 km obtained for the situation shown in Figure 4

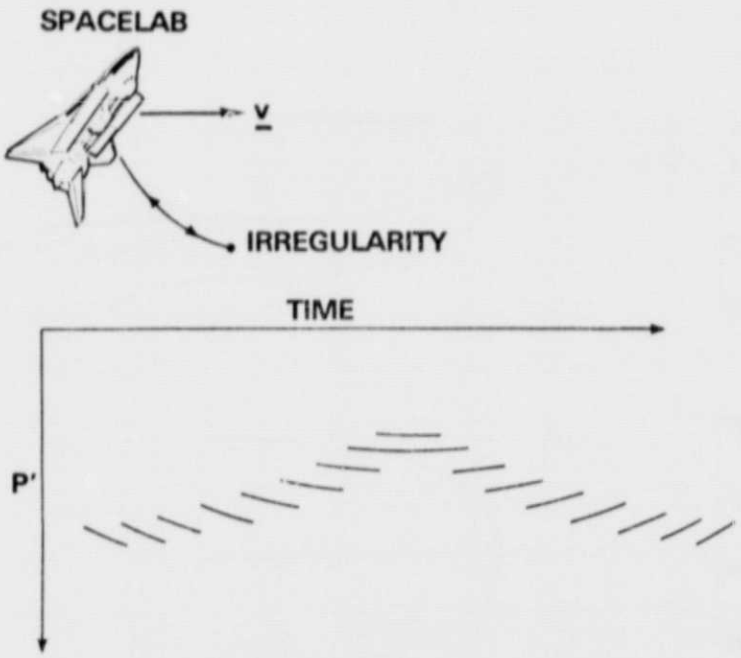

Figure 6. Doppler coded P' vs. t signature produced by an irregularity embedded in the ionosphere below Spacelab

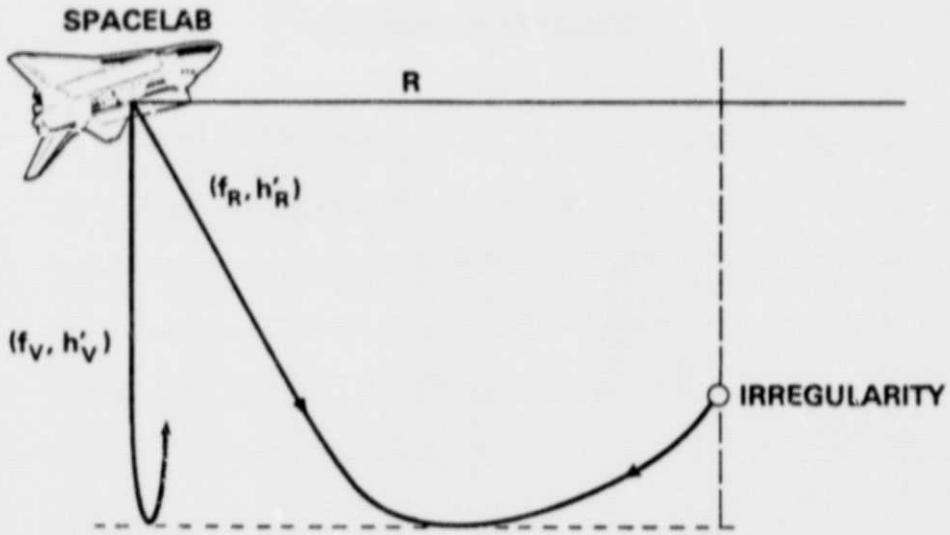

Figure 7. Ray paths having related delays and frequencies as given by Calvert and Cohen (1961)

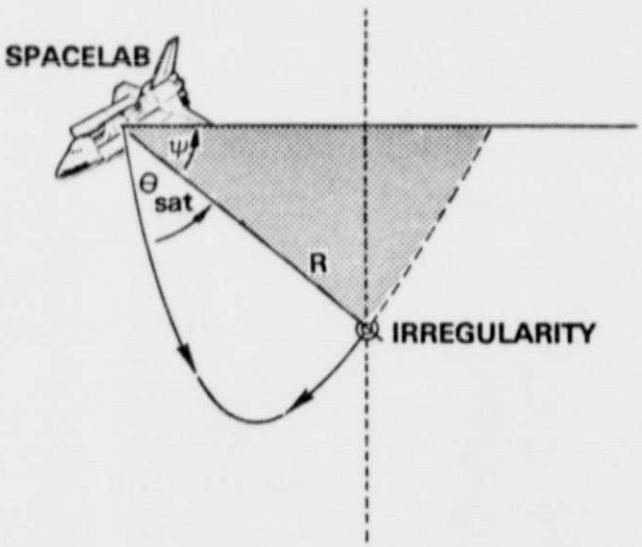

Figure 8. Ray path geometry for an irregularity displaced from the orbital plane

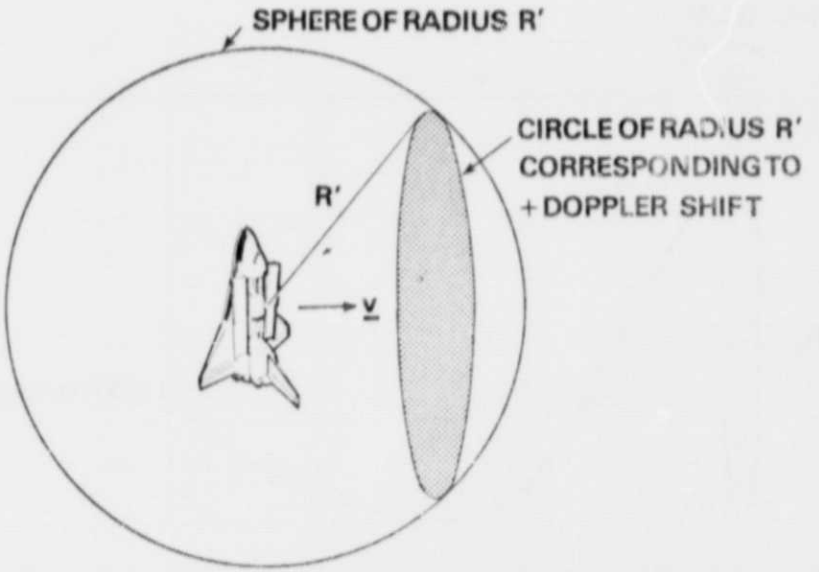

Figure 9. Echo surface determined from monostatic group delay and angle of arrival (Doppler) measurements

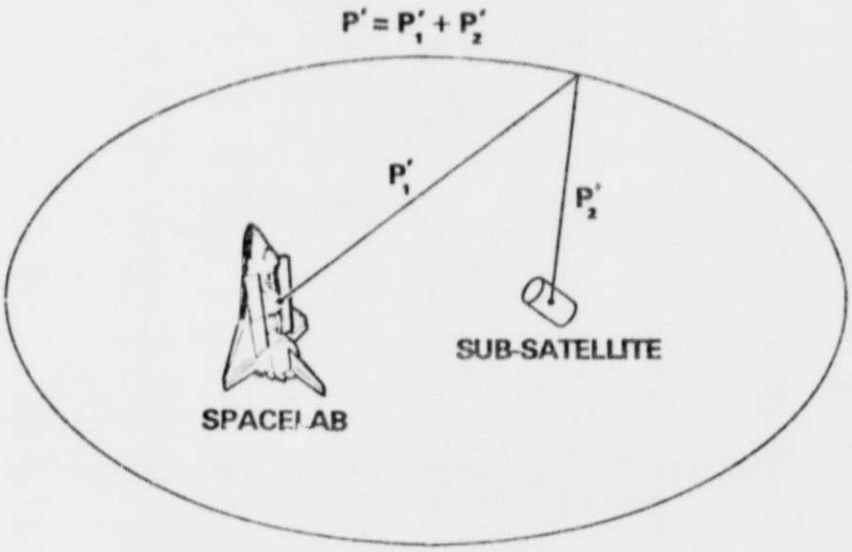

Figure 10. Echo surface defined by the group delay from Spacelab to a sub-satellite

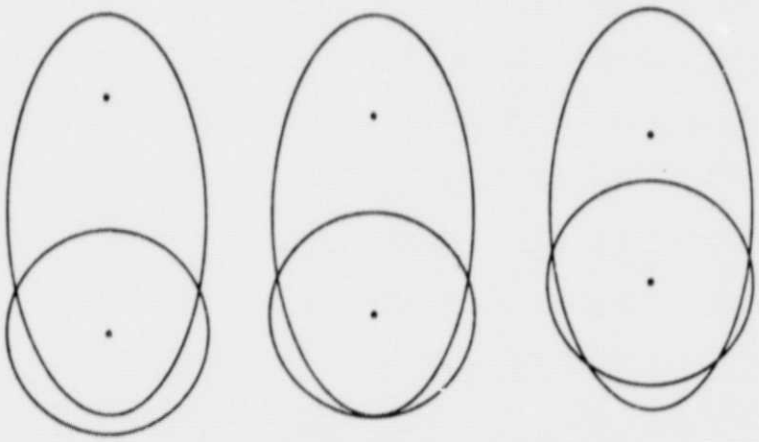

Figure 11. Intersections of monostatic and bistatic echo surfaces

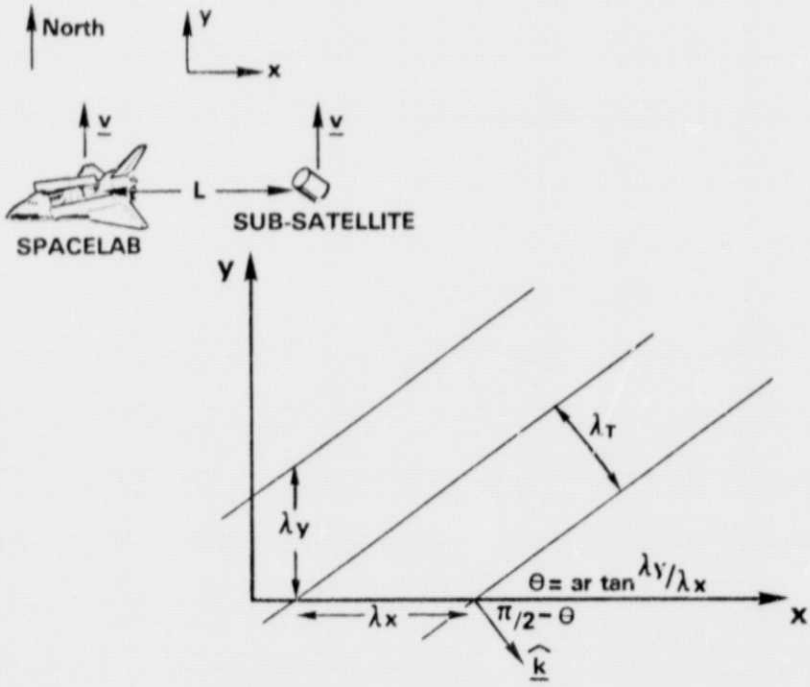

Figure 12. Geometry for Spacelab and a sub-satellite moving northward through a region containing a gravity wave